The Dominant Cutoff Wavelength of a Lunar Line*

A. Y. HU†, MEMBER, IRE, AND A. ISHIMARU‡, MEMBER, IRE

Summary—A method is presented for calculating the lowest cutoff wavelength of a new microwave transmission line, the "lunar line," which is formed by two eccentric circular metal tubes connected with a metal bar or tangential to each other. The lunar-shaped cross section is approximated by introducing a series of steps in the outer guide wall and by dividing the cross section into m fan-shape regions. Thus, the problem is reduced to one of a multiple-step waveguide and can be solved by introducing the angular parameter α_i for the individual regions. The radial boundary conditions require a combination of Bessel functions of noninteger order for each region. The common boundaries between regions give m integral equations that represent the total power in one region transferred into the next region. The integral equations are solved approximately by solving only the first terms of an infinite series expansion of the tangential electric field at the common boundary. The solution of the m-stepped waveguide results in a system of $2m$ equations containing $2m$ unknowns: the cutoff wave number β_c, the order of the Bessel function p_i, and the angular parameter α_i. A successive approximation method is applied to obtain the cutoff wavelength. The calculated value is in close agreement with experimental results.

I. Introduction

IN 1959 a new microwave transmission line, the "lunar line," was developed at The Boeing Airplane Company. The lunar line is an eccentric version of Schelkunoff's coaxial cylinders with a radial baffle[1] and is formed by two eccentric circular metal tubes which are either connected with a metal bar or are tangential to each other (Figs. 1 and 2). The cutoff frequency of the lunar line is lower than that of circular or coaxial waveguides with the same outside diameter, propagating TE_{11} mode. Its low impedance and wide bandwidth characteristics may make it useful as a transmission line, a filter, a cavity, or a feeder for an array of slot antennas.

Conventional methods of determining the cutoff wavelength cannot be applied to lunar line because of its complicated cross section. In 1958 Iashkin[2–4] proposed a new method for determining the dominant cutoff frequencies of waveguides with triangular and trapezoidal cross sections. He approximated the cross section with a series of steps and introduced new angular parameters α_i which reduced the problem to a simple system of equations. However, because his solution is restricted to a waveguide which can be approximated by multistepped rectangular regions, it cannot be applied directly to the lunar line which has circular boundaries.

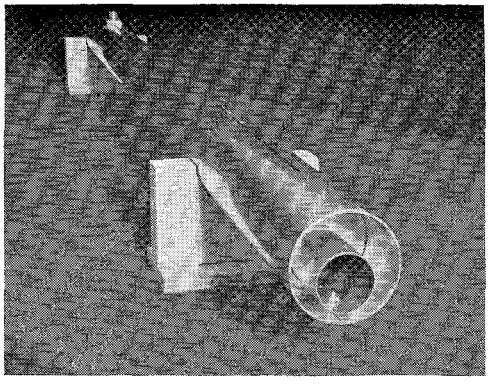

Fig. 1—Photograph of a lunar line.

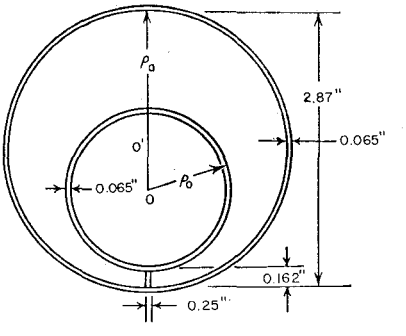

$\rho_a = 1.8955$ inches $\rho_0 = 0.8125$ inches

Fig. 2—Cross section of a lunar line.

In this paper, Iashkin's method is extended to waveguides with circular boundaries. A system of equations involving the cutoff wave number β_c, the order of the Bessel function p_i, and the angular parameter α_i, is obtained and solved approximately. The numerically calculated cutoff wavelength of the lunar line is in close agreement with experimental results.

II. Statement of the Problem

Consider the lunar line with the cross section shown in Fig. 2. It is assumed that only the dominant TE mode is propagating, and that the guide wall is perfectly conducting. The z component of the magnetic field, H_z, perpendicular to the cross section of the lunar line,

* Received by the PGMTT, May 8, 1961; revised manuscript received, July 26, 1961. The work was performed under Contract No. AF 19(604)-6189 with the AF Cambridge Res. Center, Bedford, Mass., Rept. No 1, February, 1961.

† Boeing Airplane Co., Transport Div., Renton, Wash.
‡ Dept. of Elec. Engrg., Univ. of Washington, Seattle, Wash.

[1] S. A. Schelkunoff, "Electromagnetic Waves," D. Van Nostrand Co., Inc., New York, N. Y., p. 392; 1943.

[2] A. I. Iashkin, "A method of approximate calculation for waveguides of triangular and trapezoidal cross-section," *Radiotekhnika, USSR*, vol. 3, pp. 1–9; 1958.

[3] A. I. Iashkin, "A method of approximate calculation of waveguides with complicated cross-sectional form," *Radiotekh. i elektron., USSR*, vol. 3, pp. 831–833; 1958.

[4] A. I. Iashkin, "The calculation of the fundamental critical wavelength for a rectangular waveguide with longitudinal rectangular channels and ridges," *Radiotekhnika, USSR*, vol. 13, pp. 8–14; 1958.

satisfies the two-dimensional wave equation

$$(\nabla_t^2 + \beta_c^2)H_z = 0; \quad \frac{\partial H_z}{\partial n} = 0 \text{ on the boundary,} \quad (1)$$

where ∇_t is the gradient operator transverse to the z axis, β_c is the cutoff wave number, and the cutoff wavelength is given by $\lambda_c = (2\pi/\beta_c)$.

III. Approximation by Multistepped Regions

With conventional methods, it is not possible to obtain an exact solution for (1) when it pertains to the lunar shaped region shown in Fig. 2. An approximate solution can be obtained by deforming the outer boundary of the cross section into a series of steps (Fig. 3). If the deformations are not large and have alternate signs, their effect will be negligible, and the cutoff wavelength of the original lunar line will be approximately the same as that of a waveguide with a multistepped cross section. Thus, the problem is reduced to one of finding the cutoff wavelength of the multistepped waveguide. The precision of the calculated cutoff wavelength depends on the number of steps in the cross section.

IV. Solution by Means of the Parameters α_i

The lunar line shown in Fig. 3 is deformed by eighteen fan-shape regions. Because of their symmetry about $\phi = \pi$, only nine of the eighteen regions must be considered. For a cylindrical coordinate system, the ith region is defined by

$$\phi_{i-1} \leqq \phi \leqq \phi_i,$$

$$\rho_0 \leqq \rho \leqq \rho_i,$$

where

$$i = 1, 2, \cdots 9.$$

The solution of (1) for each region is[5]

$$H_{z_i} = \sum_{n=1}^{\infty} C_{in} Z_{p_{in}}(\beta_c \rho) \cos p_{in}(\phi - \alpha_{in}), \quad (2)$$

where p is the order of the Bessel function and C is the coefficient of the series solution. The function Z_p represents the following combination of Bessel functions:

$$Z_{p_{in}}(\beta_c \rho) = J_{p_{in}}'(\beta_c \rho_0) N_{p_{in}}(\beta_c \rho) - N_{p_{in}}'(\beta_c \rho_0) J_{p_{in}}(\beta_c \rho). \quad (3)$$

Application of the boundary condition yields

$$\left.\frac{\partial H_{z_i}}{\partial \rho}\right|_{\rho=\rho_i} = 0, \quad \text{or} \quad Z_{p_{in}}'(\beta_c \rho_i) = 0 \quad (4)$$

[5] N. Marcuvitz, "Waveguide Handbook," McGraw-Hill Book Co., Inc., New York, N. Y., pp. 66–80; 1951.

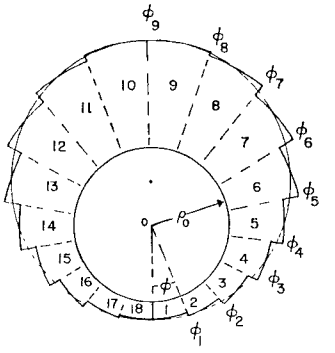

$\rho_0 = 0.8125$ inches
ρ_i = length from center o to outside of ith fan-shape region

$\rho_1 = 0.98$ inches	$\phi_1 = 20°$
$\rho_2 = 1.04$ inches	$\phi_2 = 40°$
$\rho_3 = 1.12$ inches	$\phi_3 = 60°$
$\rho_4 = 1.23$ inches	$\phi_4 = 80°$
$\rho_5 = 1.36$ inches	$\phi_5 = 100°$
$\rho_6 = 1.53$ inches	$\phi_6 = 120°$
$\rho_7 = 1.68$ inches	$\phi_7 = 140°$
$\rho_8 = 1.81$ inches	$\phi_8 = 160°$
$\rho_9 = 1.86$ inches	$\phi_9 = 180°$

Fig. 3—Cross section of an 18-stepped form of a lunar line.

and

$$\left.\frac{\partial H_{z_1}}{\partial \phi}\right|_{\phi=0} = 0, \quad \text{so} \quad \alpha_{in} = 0. \quad (5)$$

The fields must be continuous across the common boundary between the i and the $i+1$ regions $(\rho_0 \leqq \rho \leqq \rho_i, \phi = \phi_i)$; thus

$$\sum_{n=1}^{\infty} C_{in} Z_{p_{in}}(\beta_c \rho) \cos p_{in}(\phi_i - \alpha_{in}) = \sum_{n=1}^{\infty} C_{(i+1)} Z_{p(i+1)_n}(\beta_c \rho) \cos p_{(i+1)n}[\phi_i - \alpha_{(i+1)n}] \quad (6)$$

and

$$\sum_{n=1}^{\infty} C_{in} \frac{1}{\rho} p_{in} Z_{p_{in}}(\beta_c \rho) \sin p_{in}(\phi_i - \alpha_{in}) = \sum_{n=1}^{\infty} C_{(i+1)n} \frac{1}{\rho} p_{(i+1)} Z_{p(i+1)_n}(\beta_c \rho) \sin p_{(i+1)n}[\phi_i - \alpha_{(i+1)n}] = \Phi_i(\rho). \quad (7)$$

The unknown function $\Phi_i(\rho)$ is the radial electric field of the ith region. Expressed in a series form, $\Phi_i(\rho)$ is

$$\Phi_i(\rho) = \sum_{n=1}^{\infty} D_{in} \frac{Z_{p_{in}}(\beta_c \rho)}{\rho}. \quad (8)$$

The first approximation may be obtained by taking the first term of the expansion

$$\Phi_i(\rho) = D_{i1} \frac{Z_{p_{in}}(\beta_c \rho)}{\rho}. \quad (9)$$

The function $Z_{p_{in}}$ has the following properties:[6]

$$\int_{\rho_0}^{\rho_i} Z_{p_{in}}(\beta_c\rho)Z_{p_{i\nu}}(\beta_c\rho)\frac{d\rho}{\rho} = 0, \qquad \text{for } n \neq \nu, \tag{10}$$

$$\int_{\rho_0}^{\rho_i} Z_{p_{in}}{}^2(\beta_c\rho)\frac{d\rho}{\rho} = \frac{1}{2p_{in}}\left[I_{p_{in}}(\rho_i) - I_{p_{in}}(\rho_0)\right], \qquad \text{for } n = \nu. \tag{11}$$

The functions $Z_{p_{in}}$ are orthogonal in ith region. This orthogonality property can be used to determine C_{in} and $C_{(i+1)n}$ from (7) in terms of the integral involving the $\Phi(\rho)$ function. Thus

$$C_{in} = \frac{2\int_{\rho_0}^{\rho_i}\Phi_i(\xi)Z_{p_{in}}(\beta_c\xi)d\xi}{\sin p_{in}(\phi - \alpha_{in})\left[I_{p_{in}}(\rho_i) - I_{p_{in}}(\rho_0)\right]}, \tag{12}$$

$$C_{(i+1)n} = \frac{2\int_{\rho_0}^{\rho_i+1}\Phi_{i+1}(\xi)Z_{p_{(i+1)_n}}(\beta_c\xi)d\xi}{\left\{\sin p_{(i+1)n}\left[\phi - \alpha_{(i+1)n}\right]\right\}\left\{I_{p_{(i+1)_n}}\left[\rho_{(i+1)}\right] - I_{p_{(i+1)n}}(\rho_0)\right\}}. \tag{13}$$

Substituting C_{in} and $C_{(i+1)n}$ into (6) and simplifying yields the following integral equation:

$$\sum_{n=1}^{\infty}\frac{\cot p_{in}(\phi_i - \alpha_{in})\int_{\rho_0}^{\rho_i}\Phi_i(\xi)Z_{p_{in}}(\beta_c\xi)Z_{p_{in}}(\beta_c\rho)d\xi}{I_{p_{in}}(\rho_i) - I_{p_{in}}(\rho_0)}$$

$$= \sum_{n=1}^{\infty}\frac{\cot p_{(i+1)n}\left[\phi_i - \alpha_{(i+1)n}\right]\int_{\rho_0}^{\rho i+1}\Phi_{i+1}(\xi)Z_{p_{(i+1)_n}}(\beta_c\xi)Z_{p_{(i+1)_n}}(\beta_c\rho)d\xi}{I_{p_{(i+1)_n}}(\rho_{i+1}) - I_{p_{(i+1)_n}}(\rho_0)}. \tag{14}$$

The limits of the right side of the integral in (14) are $\rho_0 \rightarrow \rho_{i+1}$, but at $\phi = \phi_i$ and at $\rho_i \leqq \rho \leqq \rho_{i+1}$, the function $\Phi(\xi) = \partial H_z/\partial n = 0$. Therefore the limits change to $\rho_0 \rightarrow \rho_i$.

Eq. (14) is an integral equation for the unknown function $\Phi(\xi)$ and insures the continuity of the z component of the magnetic field at the boundary. Therefore, the unknown functions $\Phi_i(\xi)$ and $\Phi_{i+1}(\xi)$ are equal at the common boundary, and the function $\Phi_i(\xi)$ is used for a small region.

The equation which determines the cutoff wave number can be obtained by multiplying both sides of (14) by $\Phi_i(\rho)$ and by integrating over the boundary ρ_0 to ρ_i. Since $\Phi_i(\rho)$ is the tangential electric field and both sides of (14) are the z component of the magnetic field, this procedure insures that the total power of the ith region will be transferred into $(i+1)$th region, that is

$$\int_{\rho_0}^{\rho_i}\Phi_i(\rho)H_{z_i}(\rho)d\rho = \int_{\rho_0}^{\rho_i}\Phi_i(\rho)H_{z(i+1)}(\rho)d\rho. \tag{15}$$

[6] G. N. Watson, "A Treatise on the Theory of Bessel Functions," Cambridge University Press, Cambridge, Eng., p. 135; 1958.

Substituting (9) and (14) into (15) and integrating gives

$$\frac{\cot p_{i1}(\phi_i - \alpha_{i1})}{(2p_{i1})^2}\left[I_{p_{i1}}(\rho_i) - I_{p_{i1}}(\rho_0)\right] = \sum_{n=1}^{\infty}\frac{\cot p_{(i+1)n}\left[\phi_i - \alpha_{(i+1)n}\right]}{\left[I_{p_{(i+1)_n}}(\rho_{i+1}) - I_{p_{(i+1)_n}}(\rho_0)\right]} \cdot \left\{\left[\frac{\beta_c\rho_i Z_{p_{i1}}(\beta_c\rho_i)Z'_{p_{(i+1)_n}}(\beta_c\rho_i)}{(p_{i1})^2 - p^2_{(i+1)n}}\right]^2\right\}. \tag{16}$$

Between region 9 and 10, (16) is reduced to

$$\frac{\cot p_{91}(\phi_9 - \alpha_{91})}{(2p_{91})^2}\left[I_{p_{91}}(\rho_9) - I_{p_{91}}(\rho_0)\right] = 0, \tag{17}$$

since

$$\rho_9 = \rho_{10}, \quad \text{and} \quad Z'_{p_{10n}}(\beta_c\rho_9) = Z'_{p_{10n}}(\beta_c\rho_{10}) = 0.$$

Substituting $\phi_9 = \pi$ into (17) gives

$$p_{91}(\pi - \alpha_{91}) = \frac{\pi}{2}, \quad \text{or} \quad \alpha_{91} = \pi - \frac{\pi}{2p_{91}}. \tag{18}$$

At the boundary $\phi = \pi$, the field $E \propto \partial H_z/\rho\partial\phi$ is symmetric and the field H_z is zero. Thus, for the region represented in Fig. 3, a system of equations is obtained which consists of nine equations of type (4), eight equations of type (16), and one equation of type (18). Generally it is not possible to solve these equations because an infinite number of α_{in} and p_{in} must be determined. However, it is shown in Section V that (4) ad-

mits only one positive real root p_{i1}, and the rest of the roots are complex. The parameters p_{i1} and α_{i1} represent the dominant TE_{11} propagating mode. Therefore, an approximate solution is obtained by neglecting all of the nonpropagating modes. This approximation reduces the series in (16) to one term. Thus, eighteen equations of type (4), (16) and (18) contain eighteen unknown quantities β_c, α_2, $\cdots$ α_9, (drop the subscript one of α_{i1}) and p_{11}, $\cdots$ p_{91}.

To solve for β_c, assume an appropriate value of β_c and substitute this value into (4), (16) and (18) for calculating α_9. Two α_9 parameters are obtained for each β_c value. When the assumed value of β_c increases, the value of α_9 from (16) decreases and the value of α_9 from (18) increases. Therefore, the true value of β_c can be determined graphically from the point where the value of these two α_9 are equal.

V. Sample Calculation of the Cutoff Wavelength of a Lunar Line

In order to choose some appropriate value of β_c, a simplified case is first considered. Then the value of β_c, is varied near the chosen value to obtain the true β_c.

In the deformation from the lunar-line cross section, to a one-stepped, fan-shape region, the approximate cutoff wave number may be chosen as

$$\beta_c = \frac{2\pi}{2(\rho_{\text{average}} \times 190^\circ)} = 0.70. \tag{19}$$

The fan-shape is stretched to form a rectangular waveguide, and the dimension a is $\rho_{\text{average}} \times 190^\circ$; therefore, the cutoff wavelength is $2a$.

Substituting $\beta_c = 0.70$, into nine equations of type (4) and using the Bessel Function recurrence relations, gives

$$\begin{aligned} Z_{p_{\text{in}}}'(\beta_c\rho_i) = \tfrac{1}{4}\{ & [J_{p_{\text{in}}-1}(\beta_c\rho_0) - J_{p_{\text{in}}+1}(\beta_c\rho_0)] \\ & \cdot [N_{p_{\text{in}}-1}(\beta_c\rho_i) - N_{p_{\text{in}}+1}(\beta_c\rho_i)] \\ & - [N_{p_{\text{in}}-1}(\beta_c\rho_0) - N_{p_{\text{in}}+1}(\beta_c\rho_0)] \\ & [J_{p_{\text{in}}-1}(\beta_c\rho_i) - J_{p_{\text{in}}+1}(\beta_c\rho_i)]\}. \end{aligned} \tag{20}$$

The $Z_{p'_{\text{in}}}(\beta_c\rho_i)$ functions are symmetrical with respect to the $p_i = 0$; therefore, the equation $Z_{p'_{\text{in}}}(\beta_c\rho_i) = 0$ has one positive root, and must have an equal negative root. Since H_z is symmetric with respect to the $p_i = 0$, only the positive root p_{in} needs to be considered.

The values $\beta_c\rho_0$ and $\beta_c\rho_i$ are too small to be considered with the ordinary approximate formula for the large argument Bessel Functions. However, because the series form of these Bessel Functions converges rather rapidly, the finite terms are used for approximate computations to obtain the roots p_i and the parameters α_i of each β_c value.

The graphical method is used to plot the function $Z_{p_{\text{in}}}'(\beta_c\rho_i)$ against p_i (Fig. 4 shows 4 $Z_{p_1}'(\beta_c\rho_1)$ vs the p_1 curve) and the root, p_{11}, of (4) is 0.625. Similarly the roots p_{21} $\cdots$ p_{91} can be obtained. They are

$$\begin{aligned} p_{11} &= 0.625 & p_{61} &= 0.803 \\ p_{21} &= 0.648 & p_{71} &= 0.849 \\ p_{31} &= 0.673 & p_{81} &= 0.886 \\ p_{41} &= 0.708 & p_{91} &= 0.899. \\ p_{51} &= 0.7501 & & \end{aligned} \tag{21}$$

The curve in Fig. 4 shows only one positive real root. It is difficult to find complex roots of the equation $Z_{p_{\text{in}}}'(\beta_c\rho_i) = 0$ for a small argument. However, the high modes of the field, H_z, are assumed to attenuate very quickly. Substituting β_c, $\alpha_1 = 0$ and nine p_{i1} roots into eight equations of type (16), α_2 through α_9 are obtained: α_9 is 1.1832. If p_{91} is substituted into (18), the result, $\alpha_9 = 1.3943$, is different from that obtained by computing equations of type (16). Therefore, the value $\beta_c = 0.70$ does not satisfy this system of eighteen equations. However, if it is assumed that $\beta_c = 0.64$ and $\beta_c = 0.67$, and α parameters are computed using the same procedure as that used to compute $\beta_c = 0.70$, the data listed in Table I result.

When $\beta_c = 0.67$, the α_9 computed from equations of type (16) and that computed from (18) are close, therefore $\beta_c = 0.67$ satisfies the system of eighteen equations. However, other lower values of β_c have been computed in which the two α_9 parameters are different. Therefore,

TABLE I

Computing α_1 Parameter

	$\beta_c = 0.64$			$\beta_c = 0.67$			$\beta_c = 0.70$		
i	$\beta_c\rho_i$	$\hat{\rho}_{i1}$	α_i	$\beta_c\rho_i$	$\hat{\rho}_{i1}$	α_i	$\beta_c\rho_i$	ρ_{i1}	α_i
0	0.52			0.544375			0.56875		
1	0.6272	0.571	0	0.6566	0.599	0	0.686	0.625	0
2	0.6656	0.592	0.1365	0.6968	0.621	0.1087	0.728	0.648	0.1225
3	0.7168	0.617	0.2673	0.7504	0.642	0.1735	0.784	0.673	0.2234
4	0.7872	0.649	0.4371	0.8241	0.677	0.4787	0.861	0.708	0.4394
5	0.8704	0.687	0.6591	0.9112	0.718	0.7534	0.952	0.7501	0.6874
6	0.9792	0.735	0.9180	1.0251	0.771	1.0161	1.071	0.803	0.9342
7	1.0752	0.777	1.1512	1.1256	0.814	1.1657	1.176	0.849	1.1096
8	1.1584	0.813	1.3611	1.2127	0.851	1.2935	1.267	0.886	1.1872
9*	1.1904	0.829	1.5744	1.2462	0.863	1.3363	1.302	0.899	1.1832
9†			1.2468			1.32144			1.3943

* α_9 computing from type (16) equations.
† α_9 computing from (18).

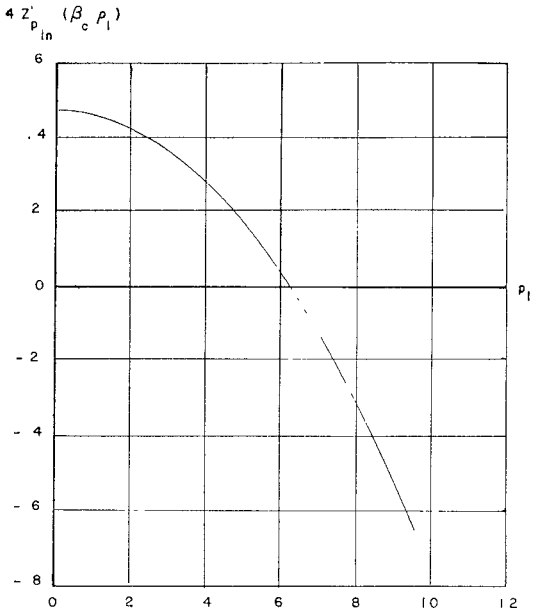

Fig. 4—$4Z'_{p_{1n}}(\beta_c p_1)$ vs p_1 curve

$\beta_c = 0.67$ is the dominant cutoff approximate wave number of the experimental lunar line. The calculated value is in close agreement with experimental results.

VI. Experimental Results

The lunar line used in the experiment was formed by two eccentric circular metal tubes, connected with a metal bar (Fig. 1). The waveguide wavelength of the lunar line was measured by the slotted section, audio-modulated signal source method. A crystal detector from an HP Model 805B slotted line was used to measure the free space wavelength λ. The crystal detector from the lunar line was used to measure the waveguide wavelength λ_g. The distance between two adjacent minimum positions indicated on the VSWR meter is equal to half a wavelength. The mean value $\lambda_g/2$ was taken as the average of four such readings. The ends of the lunar line were terminated in adjustable short circuits. Care was taken in adjusting the position of these short circuits to obtain a resonant standing wave distribution within the lunar line cavity at the measuring frequency.

The experimental result of an average cutoff wavelength of the lunar line is 9.577 inches, the cutoff wave number β_c is 0.6561.

Using the same method, the waveguide wavelengths of circular and of coaxial waveguides were measured for comparison.

For a circular waveguide of radius, $a = 1.435$ inches, a waveguide wavelength $\lambda_g = 8.52$ inches was measured at a frequency of 2800 Mc. The experimental cutoff wavelength λ_c is 4.84 inches. For a coaxial waveguide, whose outer conductor radius a is 1.435 inches and whose inner conductor radius b is 0.8125 inch, a waveguide wavelength of $\lambda_g = 8.56$ inches was measured at a frequency of 2200 Mc. The experimental cutoff wavelength λ_c is 6.8 inches. The experimental results are in close agreement with the calculated value of cutoff wavelengths for circular and coaxial waveguides. The dominant cutoff wavelength of a lunar line is lower than that of circular and coaxial waveguides having the same outside diameter.

Acknowledgment

The authors wish to express their appreciation to C. D. Lunden and D. E. Isbell for their suggestions and to acknowledge the help of the various members of the Research Unit and of the 704 Computing Unit, Transport Division, Boeing Airplane Company.